

JGR Space Physics

RESEARCH ARTICLE











10.1029/2024JA033024

One-Step Local Acceleration Process of Ultra-Relativistic Electrons in the Center of the Outer Radiation Belt: Observations



Key Points:

- Electron phase space density (PSD) radial profiles and contours are studied for ultra-relativistic electrons in September – October 2017
- Growing local peaks of PSD suggest local acceleration plays the dominant role in enhancements of ~ 7 MeV electrons in mid-September/October
- One-step local acceleration also exists for ~ 7 MeV electrons in the outer belt while previous studies put forward the two-step process

Deyu Guo¹ , Dedong Wang² , Yuri Shprits^{2,3,4} , Zheng Xiang¹ , Binbin Ni^{1,5} , Anthony Saikin⁴ , Alexander Y. Drozdov⁴ , Matyas Szabo-Roberts² , Jianhang Wang¹ , Yangxizi Liu¹, and Junhu Dong¹ 

¹Department of Space Physics, School of Electronic Information, Wuhan University, Wuhan, China, ²GFZ German Research Centre for Geosciences, Potsdam, Germany, ³Institute of Physics and Astronomy, University of Potsdam, Potsdam, Germany, ⁴Department of Earth, Planetary, and Space Science, University of California, Los Angeles, CA, USA, ⁵Chinese Academy of Sciences Center for Excellence in Comparative Planetology, Hefei, China

Supporting Information:

Supporting Information may be found in the online version of this article.

Correspondence to:

D. Wang and Z. Xiang,
dedong.wang@gfz-potsdam.de;
xiangzheng@whu.edu.cn

Citation:

Guo, D., Wang, D., Shprits, Y., Xiang, Z., Ni, B., Saikin, A., et al. (2024). One-step local acceleration process of ultra-relativistic electrons in the center of the outer radiation belt: Observations. *Journal of Geophysical Research: Space Physics*, 129, e2024JA033024. <https://doi.org/10.1029/2024JA033024>

Received 3 JUL 2024

Accepted 6 SEP 2024

Abstract Ultra-relativistic (>3 MeV) electrons are considered as a novel, separate population in the Earth's radiation belts since their loss and acceleration features are distinct from relativistic (\sim MeV) electrons. The dominant acceleration mechanism of ultra-relativistic electrons remains a subject of ongoing debate. Some studies suggest that the acceleration mechanism of ultra-relativistic electrons is energy-dependent: local acceleration dominates the enhancement of ~ 3 – 5 MeV electrons while two-step acceleration process leading by radial diffusion effects for ~ 7 MeV electrons. However, a recent study (<https://doi.org/10.1126/sciadv.abc0380>) theoretically demonstrated that local acceleration could accelerate electrons up to >7 MeV directly under the extreme plasma depletion. In this study, we report four enhancement events of ultra-relativistic electrons that occurred in September and October 2017. Analysis of phase space density (PSD) radial profiles and contours demonstrate that local acceleration plays the dominant role in the enhancements of ~ 7 MeV electrons in mid-September and mid-October, supported by persistently growing peaks in electron PSD. While enhancements of ultra-relativistic electrons in other two events still show energy-dependent phenomenon, our results provide the observation evidence that one-step local acceleration process can lead to the enhancement of ~ 7 MeV electrons in some events. We suggest that the acceleration process of ultra-relativistic electrons may be subject to the efficiency of local acceleration.

1. Introduction

The Earth's radiation belts are filled with energetic electrons trapped by the Earth's magnetic field. These high energy particles pose a hazard to the safety of astronauts and satellites working in space, as well as the communication systems of modern society (Baker, 2000, 2002; Choi et al., 2011; Li & Hudson, 2019; Love et al., 2000; Ni et al., 2016, 2022). Understanding the acceleration, loss, and transport processes that drive the dynamics of these energetic electrons has been a fundamental task in space physics research (Drozdov et al., 2021, 2022; Guo, Fu et al., 2021; Guo, Xiang et al., 2021; Millan & Thorne, 2007; Ni et al., 2008, 2013, 2017; Reeves et al., 2003; Shprits, Elkington et al., 2008; Shprits, Subbotin et al., 2008; Throne, 2010; Xiang et al., 2021).

Recent studies (Baker et al., 2014, 2019; Shprits et al., 2013, 2022; Zhao et al., 2018, 2019a) have revealed that these energetic electrons in the outer radiation zone are composed of diverse populations: relativistic (~ 500 keV – 3 MeV) electrons, and ultra-relativistic (multi-MeV, >3 MeV) electrons. While the physical processes that control the evolution of relativistic and ultra-relativistic electrons have several similarities, there are also some distinct differences between them. Examples include: (a) the loss effect of EMIC waves on ultra-relativistic electrons becomes more significant, which can produce local minima in phase space density (PSD) profiles and be responsible for narrow remnant belts, also referred to as storage rings (Baker et al., 2013; Drozdov et al., 2020; Ni et al., 2015, 2018; Shprits et al., 2013, 2016, 2017; Xiang et al., 2017, 2018); (b) the acceleration events of ultra-relativistic electrons are rarer than those of relativistic electrons, and always coincide with extremely low plasma density (Allison et al., 2021; Li et al., 2016; Shprits et al., 2022; Throne et al., 2013). These differences mentioned above suggest that it is necessary to study the main mechanism that drives the dynamics of ultra-relativistic electrons separately.

© 2024. The Author(s).

This is an open access article under the terms of the [Creative Commons Attribution License](https://creativecommons.org/licenses/by/4.0/), which permits use, distribution and reproduction in any medium, provided the original work is properly cited.

By analyzing the high-quality data measured by Van Allen Probes (also named as Radiation Belt Storm Probe, hereafter referred to as RBSP), the acceleration mechanism of ultra-relativistic electrons had been widely discussed during this decade. Reeves et al. (2013) and Throne et al. (2013) investigated the acceleration process of relativistic and ultra-relativistic electrons in October 2012 by observational analysis and simulation, showing local acceleration induced by chorus waves is the main acceleration mechanism of energetic electrons and results in local peaks in electron PSD. On the other hand, Jaynes et al. (2018) suggested that the inward radial diffusion primarily or entirely control the acceleration process of ultra-relativistic electrons up to ~ 8 MeV during the storm of 17 March 2015. Further, Zhao et al. (2018) studied the enhancement event of ultra-relativistic electrons during 21 April 2017, showing the acceleration mechanism of ultra-relativistic electrons is energy-dependent: local acceleration controls the enhancement of ~ 3 – 5 MeV electrons while radial diffusion dominant the acceleration process of ~ 7 MeV electron, demonstrating by the positive PSD radial gradient. Subsequently, the statistical study of Zhao, Baker, Li, Malaspina, et al. (2019) proposed a two-step process to explain the acceleration of ~ 7 MeV electrons: local acceleration energize electrons to relativistic and ultra-relativistic electrons beyond the RBSP's apogee, providing the source population (\sim MeV) at the high L region, further inward radial diffusion transport them to ~ 7 MeV or higher energies. The long-standing debate of the acceleration mechanism of ultra-relativistic electrons seems to be solved by energy-dependent mechanisms, where two-step process leading by inward radial diffusion dominant the enhancement of high energy electrons, such as ~ 7 MeV.

However, a recent study (Allison et al., 2021) theoretically demonstrated that local acceleration induced by chorus waves could directly energize electrons up to >7 MeV under the extreme plasma density depletion ($\sim 10 \text{ cm}^{-3}$). Thorne et al. (2013) reproduced the observed electron flux evolution of 7.15 MeV by 2-D chorus wave simulation only, provided a definitive confirmation of the dominance of chorus scattering over inward radial diffusion in causing electron acceleration during October 2012 storm. Guo et al. (2023) also pointed out that considering the energy dependence of radial diffusion coefficients (Liu et al., 2016), radial diffusion alone cannot explain the acceleration of ultra-relativistic electrons (see their Figures 4 and 5). Since the doubt upon the accuracy of the current radial diffusion coefficients remain (Lejosne & Kollmann, 2020), the main acceleration mechanism of ultra-relativistic electrons is still rife with uncertainty and doubt, particularly for the two-step acceleration process leading by inward radial diffusion on ~ 7 MeV electrons.

In this study, using the observation of Van Allen Probes *A* and *B*, we report four flux enhancement events with different strength for ultra-relativistic electrons during September and October 2017. Further we investigate PSD radial profiles and contours around the maximum values to identify its main acceleration mechanism. The result offers novel insights into the acceleration process of ultra-relativistic electrons and modify the two-step process to make it better fit with the observations. The rest of the paper is arranged as follows: Section 2 introduces the flux variation of relativistic and ultra-relativistic electrons during September and October 2017. Section 3 shows the PSD radial profiles and contours for each enhancement event of ultra-relativistic electrons and analyze the main acceleration mechanism of ultra-relativistic electrons. A discussion has been given in Section 4 to shed light upon the long-standing problem and followed by a summary in Section 5.

2. Event Overview

Figure 1 shows the evolution of energetic electron flux between September and October 2017. The first three panels show geomagnetic indexes (Kp in black and Dst in red) and solar wind parameters (dynamic pressure, solar wind speed in black and IMF Bz in red) with 1 h resolution from OMNI database. Figures 1d–1g shows the flux variations of 1.8, 3.4, 6.3 and 7.7 MeV electrons with 90° local pitch angle observed by the Relativistic Electron Proton Telescope (REPT) instrument onboard RBSP twins (Baker et al., 2012). The RBSP mission consists of two satellites which operated in a highly elliptical and low inclination orbit (Mauk et al., 2012), providing high-quality particle flux and electromagnetic wave measurement, and an excellent data set for studying the population of ultra-relativistic electrons. During this period, the apogee of RBSP orbits is located near $\text{MLT} = 10$ – 14 (not shown here). Figure 1 shows that during September and October 2017, both MeV and multi-MeV electrons undergo four significant enhancement events as a result of geomagnetic storms (see Dst index in Figure 1a), which occurred around the 8th, 15th, and 28th September and 15th October (referred to as storm 1–4 afterward), respectively. The enhancements of ultra-relativistic electrons occur slightly later than the enhancements of relativistic electrons. All of these enhancement events are characterized by high Kp values ($Kp > 4$, Figure 1a), southward IMF B_z , and high solar wind dynamic pressure and speed ($P_{\text{dyn}} > 5$ nPa, see Figure 1b, and $V_{\text{sw}} > 600$ m/s, see Figure 1c). To look into the correlation between the electron acceleration events and the depletion

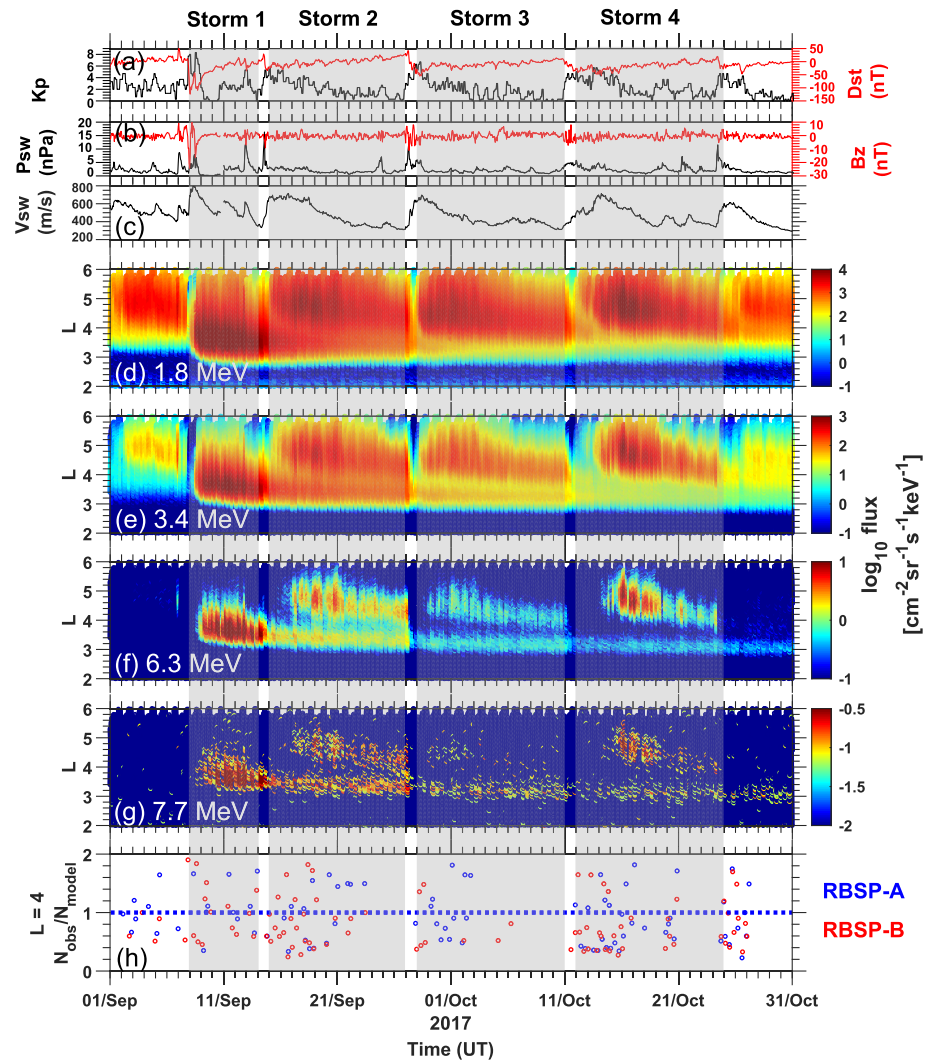


Figure 1. (a) Kp index (black line) and Dst index (red line); (b) Solar wind pressure (black line) and IMF B_z (red line); (c) Solar wind speed (d–g) Flux variation of electrons with 90° local pitch angle and different energies (1.8, 3.4, 6.3, and 7.7 MeV) observed by RBSP in September and October 2017. (h) Density ratio between averaged observation density (blue for RBSP-A and red for RBSP-B) at $L = 3.95\text{--}4.05$ in each half-orbit and the Sheeley model density (Sheeley et al., 2001) outside the plasmasphere at $L = 4$. The density ratios shown are restricted to when the averaged 1.8 MeV flux at $L = 3.95\text{--}4.05$ in each half-orbit is $> 300 \text{ cm}^{-2} \text{ s}^{-1} \text{ sr}^{-1} \text{ keV}^{-1}$. Blue dashed line represents the observation density equal to the model predicted density.

of cold plasma density, similar to Shprits et al. (2022), we show in Figure 1h the ratio between the averaged observed electron densities at $L = 3.95\text{--}4.05$ in each half-orbit and those calculated by Sheeley et al. (2001) model (RBSP-A in blue circles and RBSP-B in red circles) outside the plasmasphere at $L = 4$, restricted to time periods when the averaged flux of 1.8 MeV electrons at $L = 3.95\text{--}4.05$ in each half-orbit is larger than $300 \text{ cm}^{-2} \text{ s}^{-1} \text{ sr}^{-1} \text{ keV}^{-1}$. The plasma density is always extremely low (around 10 cm^{-3}) at the beginning of the enhancement, which creates a favorable environment for chorus waves to directly accelerate electrons up to ~ 7 MeV (Allison et al., 2021). Moreover, Figure S1 in Supporting Information S1 shows flux variations of electrons with energies from 6.3 to 15.2 MeV. The observations indicate that electron fluxes of > 7.7 MeV provided by REPT instrument are not real. The noise level from Shprits et al. (2018) is used in our study.

Around 8 September 2017, the strongest enhancement of 7.7 MeV electrons during the RBSP era occurred at relatively low L-shells ($L \sim 3.5\text{--}4$), and was then slowly transported to the lower L region. These electrons did not deplete completely through loss mechanisms acting at low L-shell, and were visible in RBSP observations for a

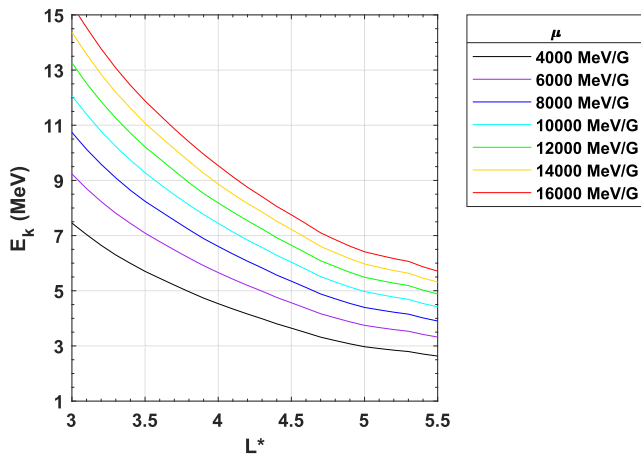


Figure 2. Averaged electron energy corresponding to $K = 0.11 \text{ G}^{1/2} R_E$, different μ values (from 4,000 to 16,000 MeV/G) as a function of L^* , calculating by the locally measured magnetic field, while K and L^* are calculated using TS04 magnetic field model (Tsyganenko & Sitnov, 2005).

long time. As a result, when the subsequent enhancements with different strength occurred, the 7.7 MeV electrons exhibited an inimitable, long-standing two-belt structure, the only one of its kind observed during the RBSP era. As a result, we chose to conduct our case study on this most intriguing time period, to see what insights we can gain into the primary acceleration mechanism responsible for these enhancement events of varying magnitudes. In this study, we conduct detailed PSD analysis by employing both the PSD profile method and PSD contour method described in the following section to ascertain the main acceleration mechanism for ultra-relativistic electrons during the studied period.

3. PSD Analysis Results

3.1. Results From PSD Profiles

To remove the adiabatic change and reveal the real acceleration of electrons during the recovery phase of storms, electron flux data from RBSP-A and RBSP-B are converted to PSD and then were interpolated to the specific μ and K . We follow the same method outlined in Allison and Shprits (2020) to calculate PSD, except that we use the TS04 magnetic field model (Tsyganenko & Sitnov, 2005) in International Radiation Belt Environment Modeling library (IRBEM, Boscher et al., 2013) to calculate K and L^* here, rather than TS07 magnetic field model (Tsyganenko & Sitnov, 2007) employed in Allison and Shprits (2020). The TS07 model is an empirical and computationally expensive model, while the TS04 model relies on the quantifiable principal magnetospheric current systems, which can be computed from the solar wind inputs. As described in Section 2, fluxes for electrons with energies larger than 7.7 MeV are not used to calculate PSD. Figure 2 shows the averaged electron energy corresponding to electrons with $K = 0.11 \text{ G}^{1/2} R_E$ and different μ values ($\mu = 4,000, 6,000, 8,000, 10,000, 12,000, 14,000$ and $16,000 \text{ MeV/G}$), calculated using the locally measured magnetic field during September and October 2017. Furthermore, the average solar wind and geomagnetic parameters during September and October 2017 are used as input for TS04 magnetic field model (Tsyganenko & Sitnov, 2005) to obtain the global magnetic fields. As shown in Figure 2, during this period, electron energy is $\sim 6.5/5.2/4.5 \text{ MeV}$ for $\mu = 8,000 \text{ MeV/G}$ and $\sim 9.5/7.5/6.3 \text{ MeV}$ for $\mu = 16,000 \text{ MeV/G}$ at $L^* = 4/4.5/5$. The electron PSD values with $K = 0.11 \text{ G}^{1/2} R_E$ and different μ values during this period are shown in Figure 3. Corresponding to the storms mentioned above, electron PSD profiles at all μ values show significant increase. However, growth of electron PSD in storm 1 is smaller than other three storms while the flux enhancement of storm 1 is the strongest in these storms. One possible explanation is that the flux enhancements of ultra-relativistic electrons occurred at lower L-shells during storm 1, thus, compared to other storms, electrons of the same μ at these L-shells correspond to higher energies and thus had lower PSD.

Figure 4 shows PSD profiles for $\mu = 8,000$ and $16,000 \text{ MeV/G}$ and $K = 0.11 \text{ G}^{1/2} R_E$ in the start of recovery phase for these four storms (7th–10th September for storm 1, 15th–18th September for storm 2, 28th September–1st October for storm 3, and 14th–17th October for storm 4). From blue to the red lines, PSD profiles over 3 days (from the end of loss/dropout to the acceleration process) are shown. Clear growing local peaks in PSD profiles for electrons with $\mu = 8,000 \text{ MeV/G}$ are observed by both RBSP-A and RBSP-B during all enhancement events at multiple orbits (at $L^* \sim 4.2$ for storm 1, corresponding to $\sim 6 \text{ MeV}$ electrons, $L^* \sim 4.7$ for storms 2, 3 and 4, corresponding to $\sim 4.9 \text{ MeV}$ electrons). This indicates that the acceleration of the electrons with energies around 5 MeV is not solely due to radial diffusion; rather, it suggests that local acceleration plays a dominant role in the enhancement process. For electrons with $\mu = 16,000 \text{ MeV/G}$ and $K = 0.11 \text{ G}^{1/2} R_E$, PSD profiles of storm 1 and 3 almost show positive gradient which may be produced by the inward radial diffusion just as mentioned in Zhao et al. (2018). However, PSD profiles of storms 2 and 4 still show growing local peaks (from the green line to the orange line) at $L^* \sim 4.7$ (corresponding $\sim 7 \text{ MeV}$ electrons), demonstrating that local acceleration also dominant the enhancement of $\sim 7 \text{ MeV}$ electrons during these periods and refutes the energy-dependent acceleration mechanism of ultra-relativistic electrons.

From an overall perspective, local peaks are more notable with the higher peak PSD value. For storms 2 and 4, local acceleration dominates the enhancement of ultra-relativistic electrons at all energies, which the maximum

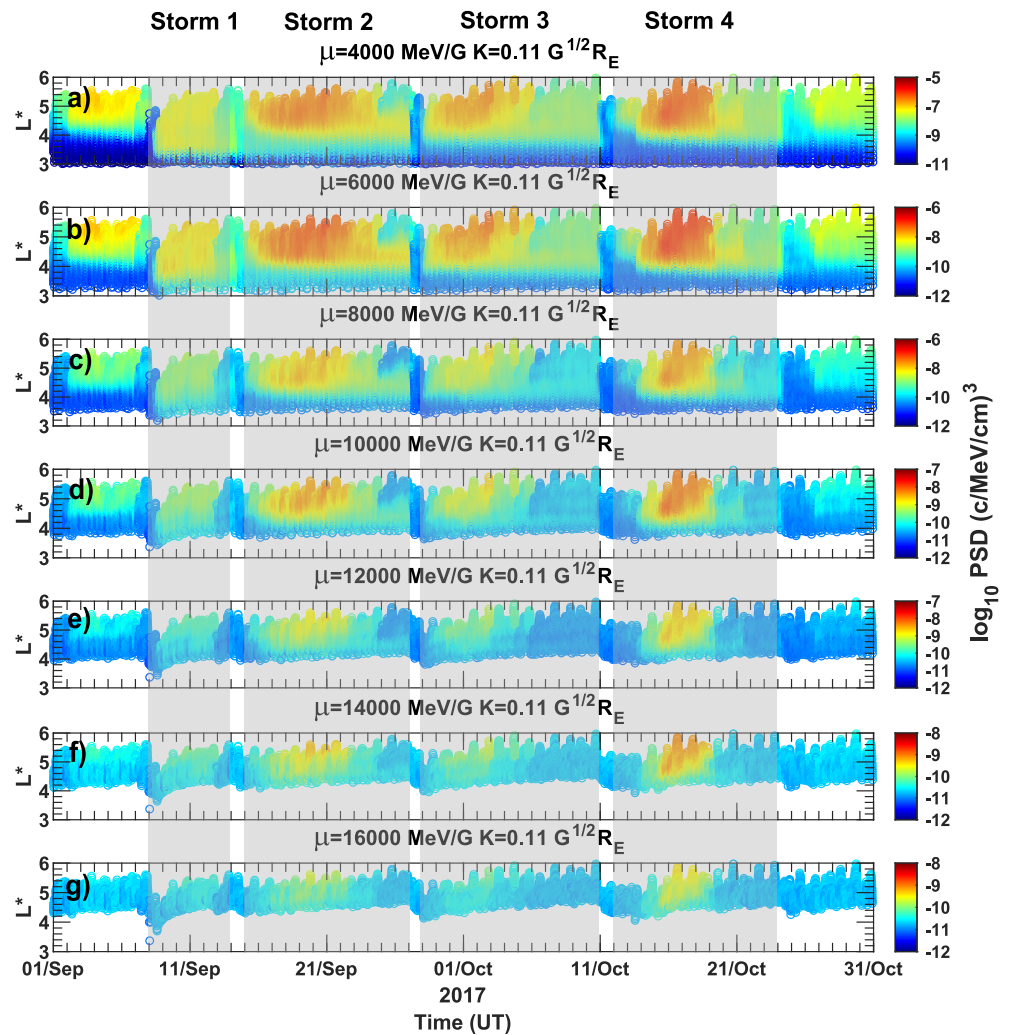


Figure 3. Phase space density values from the RBSP twins for electrons with $K = 0.11 G^{1/2} R_E$ and different μ values (4,000, 6,000, 8,000, 10,000, 12,000, 14,000, and 16,000 MeV/G) calculated using the TS04 magnetic field model during September and October 2017.

PSD values are higher than the other two storms where ~ 7 MeV electrons are energized by inward radial diffusion.

PSD profile results using the T89 and TS01 magnetic field model (Tsyganenko, 1989, 2002) are shown in Figures S2 and S3 of Supporting Information S1, which further demonstrate that the presence of growing local peaks is not sensitive to a specific magnetic field model, indicating that these local acceleration peaks are real, physical features. The presence of the local growing PSD peak suggests that ultra-relativistic electrons even for energies up to ~ 7 MeV are still dominant energized by local acceleration during the mid-September and mid-October, while for the other two storms the acceleration for high energy ultra-relativistic electrons is due to radial diffusion when the efficiency of local acceleration is insufficient.

3.2. Results From PSD Contours

Allison and Shprits (2020) proposed the PSD contour method for investigating the main mechanism of the enhancement of ultra-relativistic electrons in a more intuitive way. It should be noted that this method does not involve drawing contours of PSD, but rather outlining the area where PSD values are larger than a predetermined threshold (e.g., half an order of magnitude of the maximum PSD value). Such format allows for simultaneous

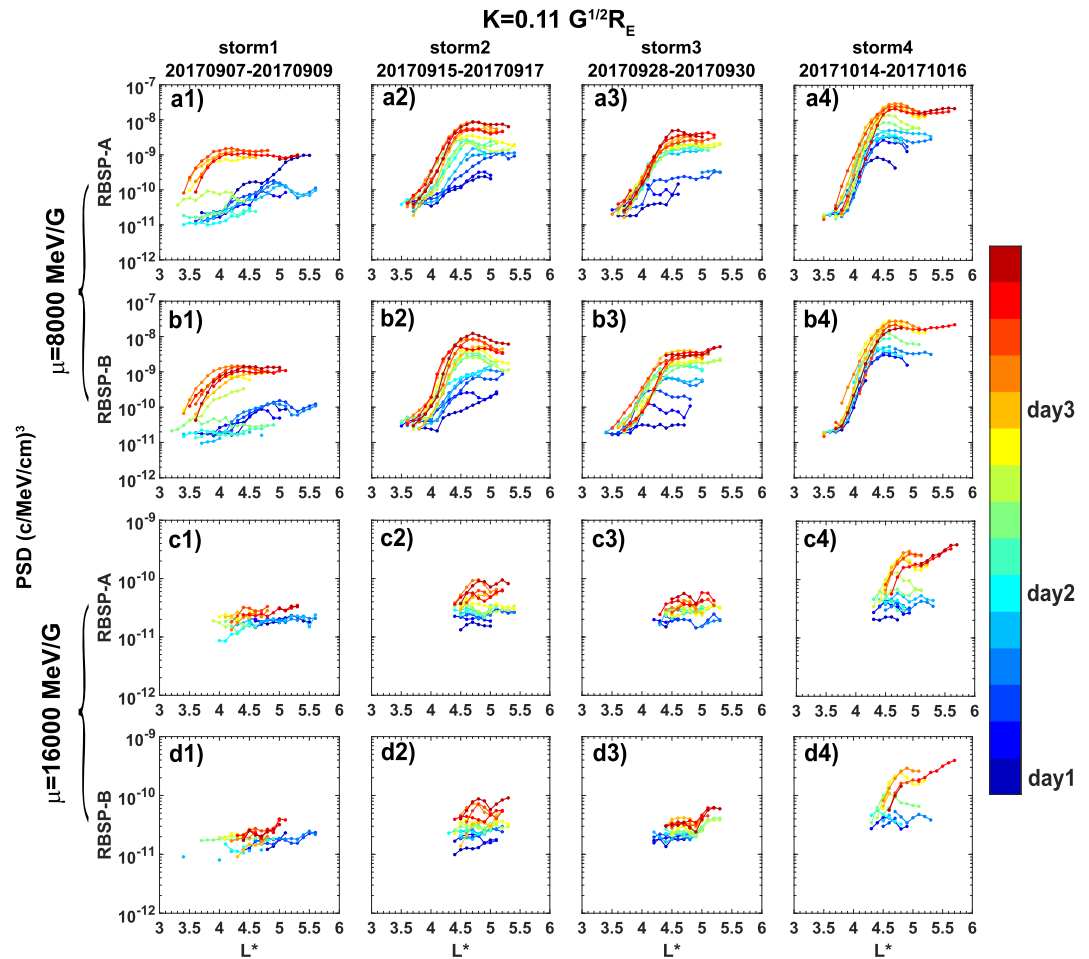


Figure 4. (a) Phase space density (PSD) radial profiles converted from fluxes observed by RBSP-A of electrons with $\mu = 8,000$ MeV/G, $K = 0.11 G^{1/2}R_E$ for recovery phases of four storms during September and October 2017, color coded by time. (b) Same as (a) but the PSD converted from fluxes observed by RBSP-B. (c–d) Same as (a) and (b) but for electrons with $\mu = 16,000$ MeV/G, $K = 0.11 G^{1/2}R_E$. K and L^* are calculated using TS04 magnetic field model while μ is calculated by locally measured magnetic field.

observation of the dynamics of the peaks in PSD at various values of the first invariant. It can also show how the energy diffusion propagates from lower energies to higher energies.

Figure 5 shows a schematic illustration of how to construct the contours around the maximum value. First, we average PSD values during each storm into 4.5 hr (around half an orbit) and 0.1 L^* bins. Black regions in Figures 5a–5d represent areas where neither RBSP-A nor -B has observations. Then, as shown with a blue star on Figure 5a, we find the maximum PSD value for electrons with a specific μ and K (e.g., $\mu = 2,000$ MeV/G and $K = 0.11 G^{1/2}R_E$) during the enhancement period. Later, regions where the PSD values are larger than the threshold (e.g., larger than half an order of magnitude below the peak value) are colored to form a contour, indicated as the blue regions in Figure 5b. Once more, we emphasize that the contour in Figure 5b does not represent the evolution of PSD, but highlights areas where PSD values are larger than the threshold, showing the regions where the high PSD values first occur. Finally, we repeat the process for other μ values keeping the same K value. For example, we do the same process for $\mu = 5,000$ MeV/G and $K = 0.11 G^{1/2}R_E$, find the maximum value shown by yellow triangle point in Figure 5c and its contour shown by yellow regions in Figure 5d. The contour figure can highlight the regions around the maximum PSD values for different μ and K , and show the evolution of the PSD peak.

Similarly to Figure 3 in Allison and Shprits (2020), illustration of the contours resulting from different mechanisms is shown in Figures 5e–5h (colors represent electrons with different μ and K), including signatures of

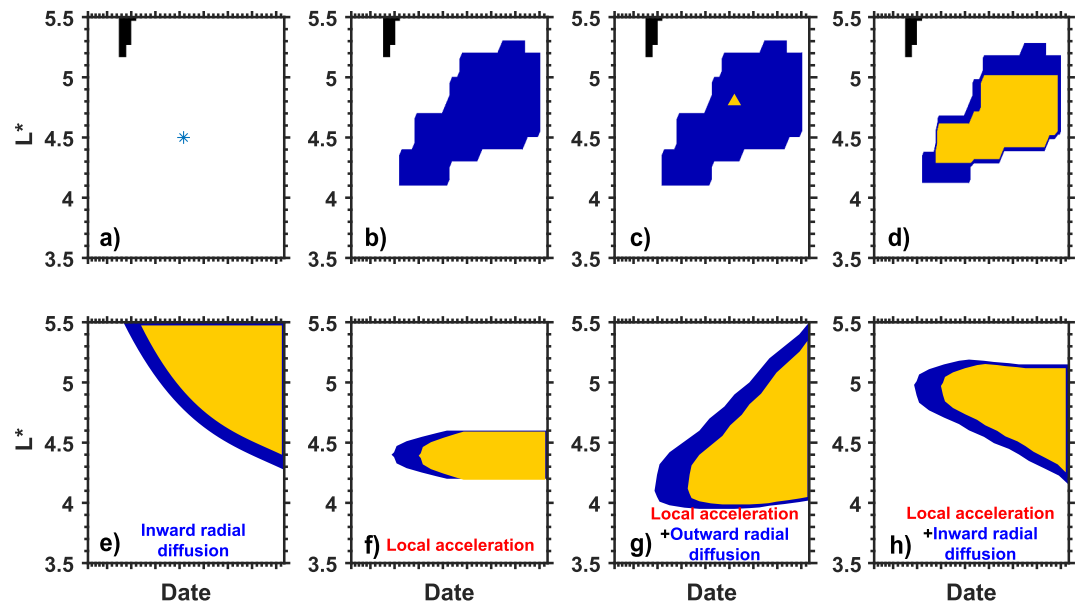


Figure 5. A schematic illustration of how to form phase space density (PSD) contours around the peak values and of the contours due to different acceleration mechanisms. To highlight areas around the peak PSD values, (a) first, we find the maximum PSD value (blue star point) for electrons with a specific μ and K value (e.g., $\mu = 2,000$ MeV/G and $K = 0.11$ G^{1/2}R_E) during a recovery phase of a storm; second, (b) plot the area where PSD values larger than thresholds (e.g., larger than the logarithmic of maximum value subtract 0.5); then, (c) find the maximum value (yellow triangle point) for electrons with another μ value keeping the same K value (e.g., $\mu = 5,000$ MeV/G and $K = 0.11$ G^{1/2}R_E); finally, (d) highlight the area where PSD values larger than thresholds. Black regions represent areas where neither RBSP-A nor -B has observations. Reproduced from Allison and Shprits (2020), ideal contours for inward radial diffusion and local acceleration are shown in (e and f), respectively. The combination of local acceleration and outward radial diffusion is shown in (g) and local acceleration coupled with inward radial diffusion in (h).

inward radial diffusion, local acceleration, a combination of local acceleration and outward radial diffusion, and a combination of local acceleration and inward radial diffusion. Figure 6a shows the PSD contour results for storm 2 (left column, 15th to 22nd September) and storm 4 (right column, 14th–20th October) with the threshold chosen as the 0.5 orders of magnitude from the maximum PSD values. Again, black regions represent areas where neither RBSP-A nor -B has observations. Figure 6b shows the Kp index, with Kp > 4 shown as red bars to highlight the disturbed periods. Figure 6c plots the chorus wave amplitudes observed by the Electric and Magnetic Field Instrument Suite and Integrated Science (EMFISIS) instrument suite (Kletzing et al., 2013). And Figure 6d shows the plasma density observations by RBSP. Note that the y-axis for Figures 6c and 6d is L* not L-shell. Around 20:00 in 16th September and 14th October, RBSP A and B observed strong chorus waves around L* ~ 4.5–5.5. Accompanied by extremely low plasma densities (~10 cm⁻³), this creates ideal conditions for electrons to be accelerated to ultra-relativistic energies during these disturbed time periods. Clear local peaks in contours of storm 4 can be found at L* ~ 4.7 (shaded area) after several hours of acceleration (see Figure 6a2). The plot shows that electron PSD at L* ~ 4.7 is larger than the chosen threshold, while electron PSD at higher L* (e.g. L* = 5) is still smaller than the threshold in the shaded period. The shape of the PSD contour is similar as Figure 5g which suggests local acceleration and subsequent outward radial diffusion. Therefore, it can be inferred that this enhancement event is dominantly caused by local acceleration at L* ~ 4.7, and then electrons are transported by radial diffusion to higher and lower L* regions. For storm 2, PSD contours also have local peaks in the shaded area. Unfortunately, the local peak has discontinuity and is not as pronounced as during storm 4, possibly due to the influence of the loss mechanism of ultra-relativistic electrons.

The PSD contour results for the storm 1 and 3 are shown in Figure 7. The pink dashed lines represent the last closed drift shell (LCDS). Extremely low plasma densities, and considerable chorus wave amplitudes are observed before the appearance of the contours by RBSP for each storm. However, while contours in storms 2 and 4 show clearly local peaks and demonstrate that these ultra-relativistic electrons up to ~7 MeV are accelerated by one-step local acceleration directly, chaotic contours in storm 1 and 3 suggest the efficiency of local acceleration

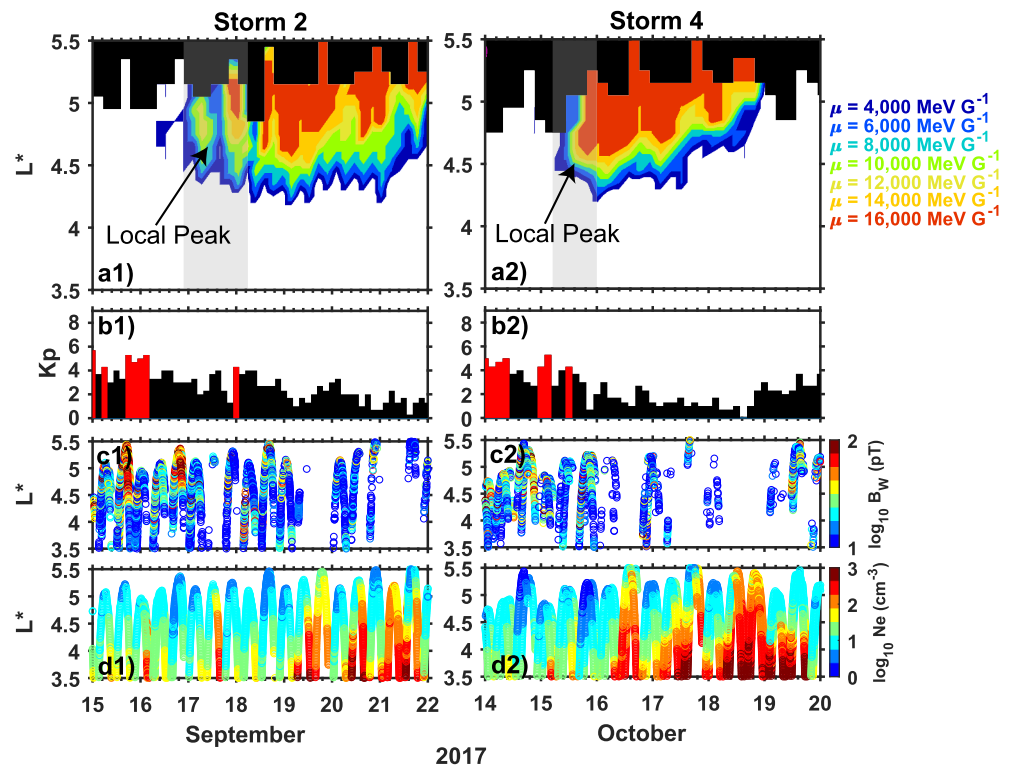


Figure 6. Left column for storm 2 (15th to 22nd September) and right column for storm 4 (14th to 20th October): (a) phase space density (PSD) contours show the L^* extent of PSD values that are within 0.5 orders of magnitude of the maximum PSD for each μ during the plot period (color coded by μ ranging from 4,000 to 16,000 MeV G^{-1}). To form the contours, the PSD values of RBSP twins were binned into 4.5 hr intervals and by 0.1 L^* . L^* values not sampled by RBSP twins are shown in black. (b) Kp index. $Kp < 4$ is shown as black bars and $Kp \geq 4$ as red bars to highlight periods of geomagnetic disturbance. (c) Chorus wave amplitudes and (d) Observation density by RBSP twins. Black regions represent areas where neither RBSP-A nor -B has observations.

maybe not sufficient enough to directly energize electrons to ~ 7 MeV or higher energy in some event even with the presence of considerable chorus wave intensity and low plasma density.

4. Discussion

By analyzing PSD radial profiles and contours of four acceleration events of ultra-relativistic electrons during September and October 2017, we provide clear observational evidence that ~ 7 MeV electrons could be energized by one-step local acceleration. There are still several points that need to be emphasized to make the reader understand this article better.

First, our study aims to provide the observational evidence that local acceleration could directly energized electrons up to ~ 7 MeV at the center of outer belt ($L^* \sim 3-5$). It has been suggested that a two-step scenario is responsible for the acceleration of MeV electrons, in which both local acceleration and radial diffusion contribute to the acceleration process. In that case, local acceleration induced by chorus waves is considered as the dominant mechanism as the illustration shown in Jaynes et al. (2015) (see Figure 1 in their study). However, the acceleration mechanism for ultra-relativistic electrons seems different. Although Zhao, Baker, Li, Malaspina, et al. (2019) proposed a two-step acceleration process for ultra-relativistic electrons, they suggest the acceleration mechanism of ultra-relativistic electrons is energy-dependent and emphasize that the radial diffusion is responsible for ~ 7 MeV electrons. Their two-step process aims to describe that radial diffusion is the direct reason of the high energy electrons (like ~ 7 MeV electrons) arise in the $L^* \sim 3-5$. Local acceleration just provides the source population for further being energized to ~ 7 MeV by radial diffusion. Storms 1 and 3 in our study confirm this two-step process in some event where enhancements of ~ 7 MeV electrons are energized by radial diffusion and local acceleration do not directly accelerate electrons up to ~ 7 MeV. Meanwhile, storm 2 and 4 demonstrate that

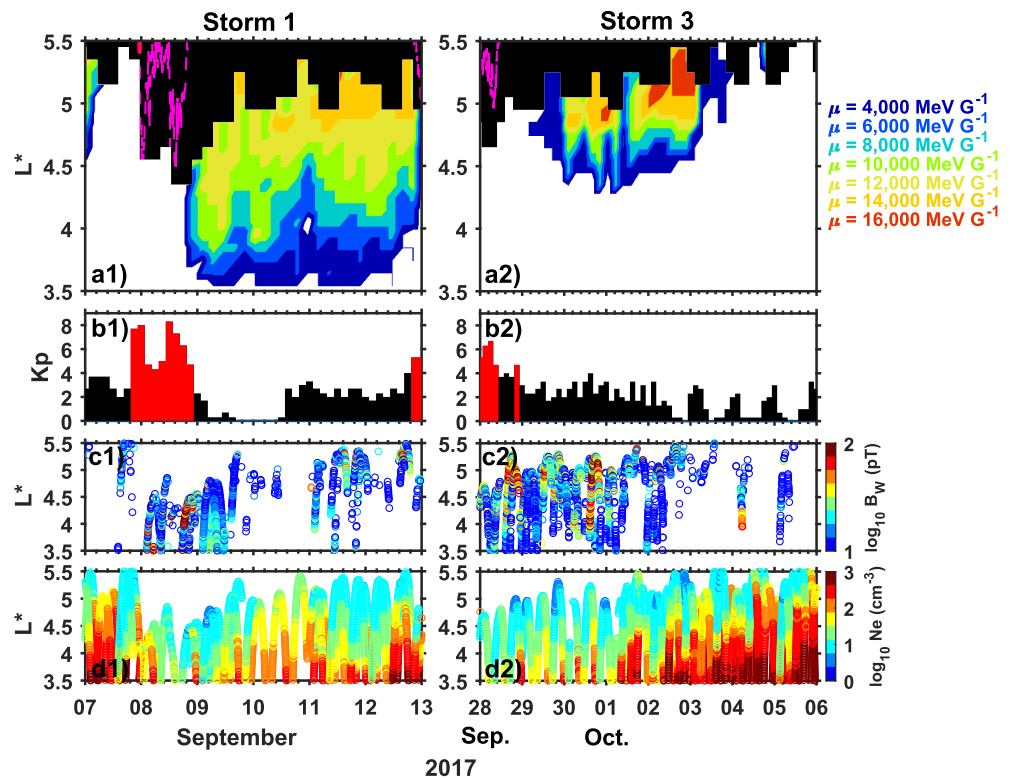


Figure 7. Same as Figure 6 but left column for storm 1 (7th to 13th September) and right column for storm 3 (28th September to 06th October). The pink dashed lines represent the last closed drift shell (LCDS).

energetic electrons can be locally accelerated to ultra-relativistic electrons in some case. One-step local acceleration could directly accelerate electrons up to ~ 7 MeV at the center of outer radiation belt, forming a rising peak structure of electron PSD. Radial diffusion, as a transport mechanism, redistributes electrons subsequently and have a minor contribution to the flux enhancement since the radial diffusion coefficient is also elevated during disturbed times (Ma et al., 2018).

Second, the enhancement process of ultra-relativistic electrons, especially for ~ 7 MeV, is subject to the efficiency of local acceleration. The enhancement of electron flux and PSD for ~ 7 MeV in storms 2 and 4 which are dominant by local acceleration is larger than the enhancement in storm 3 dominated by radial diffusion. It shows that local acceleration could cause stronger acceleration of ultra-relativistic electrons with increased space weather risk. Interestingly, there is no significant flux enhancement ($>10^{-1.5} \text{ cm}^{-2} \text{ sr}^{-1} \text{ s}^{-1} \text{ keV}^{-1}$) for the 7.7 MeV electrons from 27th–31st October between $L = 3.2\text{--}6.0$, despite similar conditions mentioned above (low plasma density, high Kp index, southward IMF B_z , and high solar wind pressure). One possible explanation is that RBSP did not observe significant chorus waves during this recovery phase of the storm. At the end of October, only electrons with energies of 1.8 and 3.4 MeV (see Figures 1c and 1d) show slight enhancements while fluxes of >6 MeV electrons are still smaller than background values (see Figures 1e and 1f). We emphasize that radial diffusion alone could not effectively accelerate electrons to ultra-relativistic electrons. Local acceleration induced by wave-particle interaction plays a major role in the process of electron acceleration and determine the strength and main energy range of electron enhancement. Radial diffusion, as a transporting mechanism, redistributes electrons and usually leads to extra weak enhancement for electrons during the process of inward diffusion while it also can infrequently produce fast and intense enhancements of ultra-relativistic electrons under extreme condition (Jaynes et al., 2018). In a word, acceleration process of ultra-relativistic electrons is subject to the efficiency of local acceleration.

Finally, PSD analysis suggests that adiabatic change may plays an important role in the enhancements of ultra-relativistic electrons. Moreover, loss mechanisms also could affect the process of acceleration (such as in storm 2, PSD contours have several gaps which may be caused by loss mechanisms). Further studies in the future need to

involve multi acceleration, loss, and transport mechanisms to reproduce and predict the evolution of ultra-relativistic electrons.

5. Summary

In this study, we report four enhancement events of ultra-relativistic electrons during four geomagnetic storms in September and October 2017. Two-belt structure of ultra-relativistic electrons is formed during this period. By analyzing both PSD profiles and PSD contours around the maximum PSD value, our results demonstrate that enhancements of electrons with ~ 7 MeV during the mid-September and mid-October are dominated by one-step local acceleration directly, with the signature growing local PSD peak being observed across multiple satellite orbits during the acceleration process. Acceleration process of ultra-relativistic electrons is subject to the efficiency of local acceleration while radial diffusion could be the direct reason for small enhancements of high energy electrons with source population providing by inefficiency local acceleration.

Data Availability Statement

Part of the software associated with the manuscript for the calculation of the IRBEM library is available in Boscher et al. (2013). Flux, density, and wave data of RBSP can be found at RBSP website (<https://spdf.gsfc.nasa.gov/pub/data/rbsp/>). The PSD, μ , K, and L^* data we produced from the REPT instrument data with 5-min time resolution can be found at Guo (2024).

Acknowledgments

This work was supported by the National Key R&D Program of China (2022YFF0503700), the National Natural Science Foundation of China (Grants 42025404, 42188101, 42174190), the B-type Strategic Priority Program of the Chinese Academy of Sciences (Grant XDB41000000). Dedong Wang acknowledges the funding support from the Deutsche Forschungsgemeinschaft (DFG) through the project "Understanding the Proper-ties of Chorus Waves in the Earth's Inner-magnetosphere and Their Effects on Van Allen Radiation Belt Electrons" (Chorus Waves)—WA 4323/5-1. Dr. Saikin's contribution was supported by NASA Grant (80NSSC21K1693).

References

- Allison, H. J., & Shprits, Y. Y. (2020). Local heating of radiation belt electrons to ultra-relativistic energies. *Nature Communications*, *11*(1), 4533. <https://doi.org/10.1038/s41467-020-18053-z>
- Allison, H. J., Shprits, Y. Y., Zhelavskaya, I. S., Wang, D., & Smirnov, A. G. (2021). Gyroresonant wave-particle interactions with chorus waves during extreme depletions of plasma density in the Van Allen radiation belts. *Science Advances*, *7*(5), eabc0380. <https://doi.org/10.1126/sciadv.abc0380>
- Baker, D., Jaynes, A., Hoxie, V., Thorne, R. M., Foster, J. C., Li, X., et al. (2014). An impenetrable barrier to ultrarelativistic electrons in the Van Allen radiation belts. *Nature*, *515*(7528), 531–534. <https://doi.org/10.1038/nature13956>
- Baker, D. N. (2000). The occurrence of operational anomalies in spacecraft and their relationship to space weather. *IEEE Transactions on Plasma Science*, *28*(6), 2007–2016. <https://doi.org/10.1109/27.902228>
- Baker, D. N. (2002). How to cope with space weather. *Science*, *297*(5586), 1486–1487. <https://doi.org/10.1126/science.1074956>
- Baker, D. N., Hoxie, V., Zhao, H., Jaynes, A. N., Kanekal, S., Li, X., & Elkington, S. (2019). Multiyear measurements of radiation belt electrons: Acceleration, transport, and loss. *Journal of Geophysical Research: Space Physics*, *124*(4), 2588–2602. <https://doi.org/10.1029/2018JA026259>
- Baker, D. N., Kanekal, S. G., Hoxie, V. C., Batiste, S., Bolton, M., Li, X., et al. (2012). The Relativistic Electron-Proton Telescope (REPT) instrument on board the Radiation Belt Storm Probes (RBSP) spacecraft: Characterization of Earth's radiation belt high-energy particle populations. *Space Science Reviews*, *179*(1–4), 337–381. <https://doi.org/10.1007/s11214-012-9950-9>
- Baker, D. N., Kanekal, S. G., Hoxie, V. C., Henderson, M. G., Li, X., Spence, H. E., et al. (2013). A long-lived relativistic electron storage ring embedded in Earth's outer Van Allen Belt. *Science*, *340*(6129), 186–190. <https://doi.org/10.1126/science.1233518>
- Boscher, D., Bourdarie, S., O'Brien, T. P., & Guild, T. (2013). The International Radiation Belt Environment Modeling (IRBEM) library [Dataset]. *Scientific Programming*. Retrieved from <http://sourceforge.net/projects/irbem>
- Choi, H.-S., Lee, J., Cho, K.-S., Kwak, Y.-S., Cho, I.-H., Park, Y.-D., et al. (2011). Analysis of GEO spacecraft anomalies: Space weather relationships. *Space Weather*, *9*(6), S06001. <https://doi.org/10.1029/2010SW000597>
- Drozdov, A. Y., Allison, H. J., Shprits, Y. Y., Elkington, S. R., & Aseev, N. A. (2021). A comparison of radial diffusion coefficients in 1-D and 3-D long-term radiation belt simulations. *Journal of Geophysical Research: Space Physics*, *126*(8), e2020JA028707. <https://doi.org/10.1029/2020ja028707>
- Drozdov, A. Y., Blum, L. W., Hartinger, M., Zhao, H., Lejosne, S., Hudson, M. K., et al. (2022). Radial transport versus local acceleration: The long-standing debate. *Earth and Space Science*, *9*(2), e2022EA002216. <https://doi.org/10.1029/2022EA002216>
- Drozdov, A. Y., Usanova, M. E., Hudson, M. K., Allison, H. J., & Shprits, Y. Y. (2020). The role of hiss, chorus, and EMIC waves in the modeling of the dynamics of the multi-MeV radiation belt electrons. *Journal of Geophysical Research: Space Physics*, *125*(9), e2020JA028282. <https://doi.org/10.1029/2020JA028282>
- Guo, D. (2024). On the acceleration mechanism of ultra-relativistic electrons in September and October 2017 [Dataset]. *Figshare*. <https://doi.org/10.6084/m9.figshare.24153531.v1>
- Guo, D., Fu, S., Xiang, Z., Ni, B., Guo, Y., Feng, M., et al. (2021a). Prediction of dynamic plasmamap location using a neural network. *Space Weather*, *19*(5), e2020SW002622. <https://doi.org/10.1029/2020SW002622>
- Guo, D., Xiang, Z., Ni, B., Cao, X., Fu, S., Zhou, R., et al. (2021b). Bounce resonance scattering of radiation belt energetic electrons by extremely low-frequency chorus waves. *Geophysical Research Letters*, *48*(22), e2021GL095714. <https://doi.org/10.1029/2021GL095714>
- Guo, D., Xiang, Z., Ni, B., Jin, T., Zhou, R., Yi, J., et al. (2023). Three-dimensional simulations of ultra-relativistic electron acceleration during the 21 April 2017 storm. *Journal of Geophysical Research: Space Physics*, *128*(4), e2023JA031407. <https://doi.org/10.1029/2023JA031407>
- Jaynes, A. N., Ali, A. F., Elkington, S. R., Malaspina, D. M., Baker, D. N., Li, X., et al. (2018). Fast diffusion of ultrarelativistic electrons in the outer radiation belt: 17 March 2015 storm event. *Geophysical Research Letters*, *45*(20), 10874–10882. <https://doi.org/10.1029/2018GL079786>
- Jaynes, A. N., Baker, D. N., Singer, H. J., Rodriguez, J. V., Loto'aniu, T. M., Ali, A. F., et al. (2015). Source and seed populations for relativistic electrons: Their roles in radiation belt changes. *Journal of Geophysical Research: Space Physics*, *120*(9), 7240–7254. <https://doi.org/10.1002/2015JA021234>

- Kletzing, C. A., Kurth, W. S., Acuna, M., MacDowall, R. J., Torbert, R. B., Averkamp, T., et al. (2013). The Electric and Magnetic Field Instrument Suite And Integrated Science (EMFISIS) on RBSP. *Space Science Reviews*, 179(1–4), 127–181. <https://doi.org/10.1007/s11214-013-9993-6>
- Lejosne, S., & Kollmann, P. (2020). Radiation belt radial diffusion at Earth and beyond. *Space Science Reviews*, 216(1), 19. <https://doi.org/10.1007/s11214-020-0642-6>
- Li, W., & Hudson, M. K. (2019). Earth's Van Allen radiation belts: From discovery to the Van Allen probes era. *Journal of Geophysical Research: Space Physics*, 124(11), 8319–8351. <https://doi.org/10.1029/2018JA025940>
- Li, W., Ma, Q., Thorne, R. M., Bortnik, J., Zhang, X., Li, J., et al. (2016). Radiation belt electron acceleration during the 17 March 2015 geomagnetic storm: Observations and simulations. *Journal of Geophysical Research: Space Physics*, 121(6), 5520–5536. <https://doi.org/10.1002/2016JA022400>
- Liu, W., Tu, W., Li, X., Sarris, T., Khotyaintsev, Y., Fu, H., et al. (2016). On the calculation of electric diffusion coefficient of radiation belt electrons with in situ electric field measurements by THEMIS. *Geophysical Research Letters*, 43(3), 1023–1030. <https://doi.org/10.1002/2015GL067398>
- Love, D. P., Toomb, D. S., Wilkinson, D. C., & Parkinson, J. B. (2000). Penetrating electron fluctuations associated with GEO spacecraft anomalies. *IEEE Transactions on Plasma Science*, 28(6), 2075–2084. <https://doi.org/10.1109/27.902234>
- Ma, Q., Li, W., Bortnik, J., Thorne, R. M., Chu, X., Ozeke, L. G., et al. (2018). Quantitative evaluation of radial diffusion and local acceleration processes during GEM challenge events. *Journal of Geophysical Research: Space Physics*, 123(3), 1938–1952. <https://doi.org/10.1002/2017JA025114>
- Mauk, B. H., Fox, N. J., Kanekal, S. G., Kessel, R. L., Sibeck, D. G., & Khorkorskiy, A. (2012). Science objectives and rationale for the radiation belt storm probes mission. *Space Science Reviews*, 179(1–4), 1–15. <https://doi.org/10.1007/s11214-012-9908y>
- Millan, R. M., & Thorne, R. M. (2007). Review of radiation belt relativistic electron losses. *Journal of Atmospheric and Solar-Terrestrial Physics*, 69(3), 362–377. <https://doi.org/10.1016/j.jastp.2006.06.019>
- Ni, B., Bortnik, J., Thorne, R. M., Ma, Q., & Chen, L. (2013). Resonant scattering and resultant pitch angle evolution of relativistic electrons by plasmaspheric hiss. *Journal of Geophysical Research: Space Physics*, 118(12), 7740–7751. <https://doi.org/10.1002/2013JA019260>
- Ni, B., Cao, X., Shprits, Y. Y., Summers, D., Gu, X., Fu, S., & Lou, Y. (2018). Hot plasma effects on the cyclotron-resonant pitch-angle scattering rates of radiation belt electrons due to EMIC waves. *Geophysical Research Letters*, 45(1), 21–30. <https://doi.org/10.1002/2017GL076028>
- Ni, B., Cao, X., Zou, Z., Zhou, C., Gu, X., Bortnik, J., et al. (2015). Resonant scattering of outer zone relativistic electrons by multiband EMIC waves and resultant electron loss time scales. *Journal of Geophysical Research: Space Physics*, 120(9), 7357–7373. <https://doi.org/10.1002/2015JA021466>
- Ni, B., Hua, M., Gu, X., Fu, S., Xiang, Z., Cao, X., & Ma, X. (2022). Artificial modification of Earth's radiation belts by ground-based Very-Low-Frequency (VLF) transmitters. *Science China Earth Sciences*, 65(3), 391–413. <https://doi.org/10.1007/s11430-021-9850-7>
- Ni, B., Hua, M., Zhou, R., Yi, J., & Fu, S. (2017). Competition between outer zone electron scattering by plasmaspheric hiss and magnetosonic waves. *Geophysical Research Letters*, 44(8), 3465–3474. <https://doi.org/10.1002/2017GL072989>
- Ni, B., Thorne, R. M., Shprits, Y. Y., & Bortnik, J. (2008). Resonant scattering of plasma sheet electrons by whistler-mode chorus: Contribution to diffuse auroral precipitation. *Geophysical Research Letters*, 35(11), L11106. <https://doi.org/10.1029/2008GL034032>
- Ni, B., Thorne, R. M., Zhang, X., Bortnik, J., Pu, Z., Xie, L., et al. (2016). Origins of the Earth's diffuse auroral precipitation. *Space Science Reviews*, 200(1–4), 205–259. <https://doi.org/10.1007/s11214-016-0234-7>
- Reeves, G. D., McAdams, K. L., Friedel, R. H. W., & O'Brien, T. P. (2003). Acceleration and loss of relativistic electrons during geomagnetic storms. *Geophysical Research Letters*, 30(10), 1529. <https://doi.org/10.1029/2002GL016513>
- Reeves, G. D., Spence, H. E., Henderson, M. G., Morley, S. K., Friedel, R. H. W., Funsten, H. O., et al. (2013). Electron acceleration in the heart of the Van Allen radiation belts. *Science*, 341(6149), 991–994. <https://doi.org/10.1126/science.1237743>
- Sheeley, B. W., Moldwin, M. B., Rassoul, H. K., & Anderson, R. R. (2001). An empirical plasmasphere and trough density model: CRRES observations. *Journal of Geophysical Research*, 106(A11), 25631–25641. <https://doi.org/10.1029/2000JA000286>
- Shprits, Y., Horne, R., Kellerman, A., & Drozdov, A. Y. (2018). The dynamics of Van Allen belts revisited. *Nature Physics*, 14(2), 102–103. <https://doi.org/10.1038/nphys4350>
- Shprits, Y. Y., Allison, H. J., Wang, D., Drozdov, A., Szabo-Roberts, M., Zhelavskaya, I., et al. (2022). A new population of ultra-relativistic electrons in the outer radiation zone. *Journal of Geophysical Research: Space Physics*, 127(5), e2021JA030214. <https://doi.org/10.1029/2021JA030214>
- Shprits, Y. Y., Drozdov, A. Y., Spasojevic, M., Kellerman, A. C., Usanova, M. E., Engebretson, M. J., et al. (2016). Wave-induced loss of ultra-relativistic electrons in the Van Allen radiation belts. *Nature Communications*, 7(1), 12883. <https://doi.org/10.1038/ncomms12883>
- Shprits, Y. Y., Elkington, S. R., Meredith, N. P., & Subbotin, D. A. (2008a). Review of modeling of losses and sources of relativistic electrons in the outer radiation belt. I: Radial transport. *Journal of Atmospheric and Solar-Terrestrial Physics*, 70(14), 1679–1693. <https://doi.org/10.1016/j.jastp.2008.06.008>
- Shprits, Y. Y., Kellerman, A., Aseev, N., Drozdov, A. Y., & Michaelis, I. (2017). Multi-MeV electron loss in the heart of the radiation belts. *Geophysical Research Letters*, 44(3), 1204–1209. <https://doi.org/10.1002/2016GL072258>
- Shprits, Y. Y., Subbotin, D., Drozdov, A., Usanova, M. E., Kellerman, A., Orlova, K., et al. (2013). Unusual stable trapping of the ultrarelativistic electrons in the Van Allen radiation belts. *Nature Physics*, 9(11), 699–703. <https://doi.org/10.1038/nphys2760>
- Shprits, Y. Y., Subbotin, D. A., Meredith, N. P., & Elkington, S. R. (2008b). Review of modeling of losses and sources of relativistic electrons in the outer radiation belt. II: Local acceleration and loss. *Journal of Atmospheric and Solar-Terrestrial Physics*, 70(14), 1694–1713. <https://doi.org/10.1016/j.jastp.2008.06.014>
- Thorne, R. M. (2010). Radiation belt dynamics: The importance of wave-particle interactions. *Geophysical Research Letters*, 37(22), L22107. <https://doi.org/10.1029/2010GL044990>
- Thorne, R. M., Li, W., Ni, B., Ma, Q., Bortnik, J., Chen, L., et al. (2013). Rapid local acceleration of relativistic radiation-belt electrons by magnetospheric chorus. *Nature*, 504(7480), 411–414. <https://doi.org/10.1038/nature12889>
- Tsyganenko, N. A. (1989). A magnetospheric magnetic field model with a warped tail current sheet. *Planetary and Space Science*, 37(1), 5–20. [https://doi.org/10.1016/0032-0633\(89\)90066-4](https://doi.org/10.1016/0032-0633(89)90066-4)
- Tsyganenko, N. A. (2002). A model of the magnetosphere with a dawn-dusk asymmetry, 1, Mathematical structure. *Journal of Geophysical Research*, 107(A8), SMP12-1–SMP12-15. <https://doi.org/10.1029/2001JA000219>
- Tsyganenko, N. A., & Sitnov, M. I. (2005). Modeling the dynamics of the inner magnetosphere during strong geomagnetic storms. *Journal of Geophysical Research*, 110(A3), A03208. <https://doi.org/10.1029/2004JA010798>
- Tsyganenko, N. A., & Sitnov, M. I. (2007). Magnetospheric configurations from a high-resolution data-based magnetic field model. *Journal of Geophysical Research*, 112(A6), A06225. <https://doi.org/10.1029/2007JA012260>

- Xiang, Z., Li, X., Kapali, S., Gannon, J., Ni, B., Zhao, H., et al. (2021). Modeling the dynamics of radiation belt electrons with source and loss driven by the solar wind. *Journal of Geophysical Research: Space Physics*, *126*(6), e2020JA028988. <https://doi.org/10.1029/2020JA028988>
- Xiang, Z., Tu, W., Li, X., Ni, B., Morley, S. K., & Baker, D. N. (2017). Understanding the mechanisms of radiation belt dropouts observed by Van Allen probes. *Journal of Geophysical Research: Space Physics*, *122*(10), 9858–9879. <https://doi.org/10.1002/2017JA024487>
- Xiang, Z., Tu, W., Ni, B., Henderson, M. G., & Cao, X. (2018). A statistical survey of radiation belt dropouts observed by Van Allen probes. *Geophysical Research Letters*, *45*(16), 8035–8043. <https://doi.org/10.1029/2018GL078907>
- Zhao, H., Baker, D. N., Li, X., Jaynes, A. N., & Kanekal, S. G. (2018). The acceleration of ultrarelativistic electrons during a small to moderate storm of 21 April 2017. *Geophysical Research Letters*, *45*(12), 5818–5825. <https://doi.org/10.1029/2018GL078582>
- Zhao, H., Baker, D. N., Li, X., Jaynes, A. N., & Kanekal, S. G. (2019a). The effects of geomagnetic storms and solar wind conditions on the ultrarelativistic electron flux enhancements. *Journal of Geophysical Research: Space Physics*, *124*(3), 1948–1965. <https://doi.org/10.1029/2018JA026257>
- Zhao, H., Baker, D. N., Li, X., Malaspina, D. M., Jaynes, A. N., & Kanekal, S. G. (2019b). On the acceleration mechanism of ultrarelativistic electrons in the center of the outer radiation belt: A statistical study. *Journal of Geophysical Research: Space Physics*, *124*(11), 8590–8599. <https://doi.org/10.1029/2019JA027111>